

# Polymer Chemistry

Accepted Manuscript



This article can be cited before page numbers have been issued, to do this please use: S. B. Luk, J. Kollar, A. Chovancova, M. Mrlík, I. Lacik, J. Mosnacek and R. A. Hutchinson, *Polym. Chem.*, 2017, DOI: 10.1039/C7PY01397C.



This is an Accepted Manuscript, which has been through the Royal Society of Chemistry peer review process and has been accepted for publication.

Accepted Manuscripts are published online shortly after acceptance, before technical editing, formatting and proof reading. Using this free service, authors can make their results available to the community, in citable form, before we publish the edited article. We will replace this Accepted Manuscript with the edited and formatted Advance Article as soon as it is available.

You can find more information about Accepted Manuscripts in the [author guidelines](#).

Please note that technical editing may introduce minor changes to the text and/or graphics, which may alter content. The journal's standard [Terms & Conditions](#) and the ethical guidelines, outlined in our [author and reviewer resource centre](#), still apply. In no event shall the Royal Society of Chemistry be held responsible for any errors or omissions in this Accepted Manuscript or any consequences arising from the use of any information it contains.



# Polymer Chemistry

## ARTICLE

### Superabsorbent Hydrogels made from Bio-sourced Butyrolactone Monomer in Aqueous Solution

Sharmaine B. Luk,<sup>a</sup> Jozef Kollár,<sup>b</sup> Anna Chovancová,<sup>b</sup> Miroslav Mrlík,<sup>c</sup> Igor Lacík,<sup>b</sup> Jaroslav Mosnáček,<sup>\*b</sup> and Robin A. Hutchinson<sup>\*a</sup>

Received 00th January 20xx,  
Accepted 00th January 20xx

DOI: 10.1039/x0xx00000x

www.rsc.org/

A new water-soluble monomer, sodium 4-hydroxy-4-methyl-2-methylene butanoate (SHMeMB), formed by saponification of the bio-derived monomer  $\gamma$ -methyl- $\alpha$ -methylene- $\gamma$ -butyrolactone (MeMBL), was copolymerized with acrylamide (AM) in aqueous solution to make superabsorbent hydrogels with equilibrium degree of swelling in the range of 6 700 – 59 000 %, depending on monomer ratio and crosslink density. Mechanical strength and storage and loss moduli of the hydrogels were tunable over a wide range through adjustment of the comonomer composition and the crosslinker content. Monomer reactivity ratios of  $r_{\text{SHMeMB}} = 0.12\text{--}0.17$  and  $r_{\text{AM}} = 0.95\text{--}1.10$  were determined using copolymer compositions measured at low monomer conversion as well as by applying the integrated form of the Mayo-Lewis equation to fit the drift in comonomer composition with conversion. The reactivity of the SHMeMB:AM system was lower than that of the previously-studied SHMB:AM system, with sodium 4-hydroxy-2-methylene butanoate (SHMB) derived from a similar renewable monomer,  $\alpha$ -methylene- $\gamma$ -butyrolactone (MBL). The differences in reactivity were studied by pulsed laser polymerization coupled with size exclusion chromatography; the comonomer-averaged propagation rate coefficient of the SHMB:AM system was found to be more than double that of SHMeMB:AM, with first estimates for the SHMeMB and SHMB homopropagation rate coefficients of 25 and 165 L·mol<sup>-1</sup>·s<sup>-1</sup>, respectively, at 60 °C. Despite its lower reactivity, SHMeMB offers advantages over SHMB due to its availability and as superior overall properties of the final hydrogels were achieved.

### Introduction

Water-soluble polymers are used in many applications including drug delivery,<sup>1</sup> flocculation for water recovery in oil sand tailings,<sup>2</sup> and metal ion recovery.<sup>3</sup> Synthesizing these materials in aqueous solution provides the additional benefit of eliminating the use of volatile organic compounds (VOCs) and their associated adverse impact on health<sup>4</sup> and the environment.<sup>5</sup> The environmental impact of these materials can be lessened further by using alternative and renewable feedstocks, as the extraction of crude oil also contributes to VOCs in the atmosphere<sup>6</sup> and depends largely on political and economic factors.<sup>7</sup> Some bio-sourced polymers that are currently commercialized are sugar-based poly(lactic acid)<sup>8</sup> and poly(hydroxyalkanoate),<sup>9</sup> with other bio-sourced monomers, including  $\beta$ -myrcene and limonene, that are terpene-based.<sup>10</sup>

Tulipalin A, formally known as  $\alpha$ -methylene- $\gamma$ -butyrolactone (MBL), can be derived from 6-tuliposides found in tulips at levels

of 0.2 – 2 wt%.<sup>11</sup> Alternatively, MBL can be synthesized from biomass sugar-based itaconic anhydride<sup>12</sup> or pyruvate using acetyl coenzyme A.<sup>13</sup> A similar monomer,  $\gamma$ -methyl- $\alpha$ -methylene- $\gamma$ -butyrolactone (MeMBL), has been synthesized in a catalytic two-step process using bio-derived levulinic acid.<sup>14</sup> Both monomers are lactone rings with an exocyclic double bond and have been successfully polymerized to make transparent and hard thermoplastics similar to poly(methyl methacrylate) (PMMA), but with higher glass transition temperature ( $T_g$ ) and solvent resistance.<sup>15,16</sup> While the homopolymers demonstrated promising properties, their brittleness led to a focus on copolymerization with monomers such as styrene (ST) and methyl methacrylate (MMA).<sup>17,18</sup> Both MBL and MeMBL were more reactive compared to ST, and even more so compared to MMA.

These polymerizations were all done in bulk or organic solution, with the monomers in their closed-ring form. However, it was demonstrated that PMBL could be hydrolyzed in the presence of a strong base to open the lactone ring and form poly( $\alpha$ -methylene- $\gamma$ -hydroxybutyric acid).<sup>15</sup> In the presence of potassium hydroxide at 100°C, however, the resulting polymer was not completely water-soluble and closure of the lactone rings occurred when acid was added at room temperature. Only when hydrolyzed with a very strong base, such as hydrazine, did the polymer become completely water-soluble. The disadvantage of post-polymerization saponification remains the incomplete ring-opening of the lactone rings, as also seen in

<sup>a</sup> Queen's University, Department of Chemical Engineering, 19 Division St., Kingston, Ontario, Canada, K7L 3N6

<sup>b</sup> Polymer Institute of the Slovak Academy of Sciences, Dúbravská cesta 9, 845 41, Bratislava, Slovakia

<sup>c</sup> Centre of Polymer Systems, University Institute, Tomas Bata University in Zlin, Nad Ovcirnou 3685, 760 01 Zlin, Czech Republic

\* E-mail: jaroslav.mosnacek@savba.sk; robin.hutchinson@queensu.ca  
Electronic Supplementary Information (ESI) available: [details of any supplementary information available should be included here]. See DOI: 10.1039/x0xx00000x

emulsion polymerization of MBL and acrylic acid with crosslinker saponified to make superabsorbent hydrogel particles.<sup>19</sup>

More recently, Kollár *et al.* demonstrated that saponification of MBL monomer with sodium hydroxide proceeds rapidly to form a completely water-soluble monomer.<sup>20</sup> The resulting sodium 4-hydroxy-2-methylene butanoate (SHMB) was then copolymerized with acrylamide (AM) in aqueous solution at different molar ratios in the presence of *N,N'*-methylenebis(acrylamide) (BIS) crosslinker to make superabsorbent hydrogels that exhibited a significantly higher degree of swelling in water than conventional sodium acrylate:AM hydrogel materials.<sup>20</sup> The same study also provided some information regarding the polymerization kinetics, reporting reactivity ratios of the system and also investigating SHMB homopolymerization, which was very slow compared to that of AM.

To the best of our knowledge, currently MBL is only available in small scale for research purposes and it is not extracted from renewable resources, but synthesized from petroleum based products. On the other hand, MeMBL has been synthesized more efficiently by DuPont from bio-derived sources<sup>14</sup> and the scale-up to commercial production has been investigated. Therefore, in this work, MeMBL was saponified to make sodium 4-hydroxy-4-methyl-2-methylene butanoate (SHMeMB) and copolymerized with AM and BIS crosslinker to make superabsorbent hydrogels similar to those recently produced from SHMB. Properties of the SHMeMB:AM hydrogels could not be directly compared to SHMB:AM hydrogels, due to the differences in the comonomer reactivity ratios between these two systems. This motivated further studies to understand their relative reactivity ratios using an *in-situ* NMR method previously employed to study the aqueous radical copolymerization kinetics of acrylic acid and acrylamide.<sup>21</sup> In addition, these two systems were compared using the pulsed laser polymerization coupled with size exclusion chromatography (PLP-SEC) technique, an IUPAC recommended method for determining propagation rate coefficients ( $k_p$ )<sup>22</sup> that has been used to study various water-soluble monomers such as non-ionized to fully ionized (meth)acrylic acids<sup>23-26</sup> and acrylamide.<sup>27</sup>

## Experimental

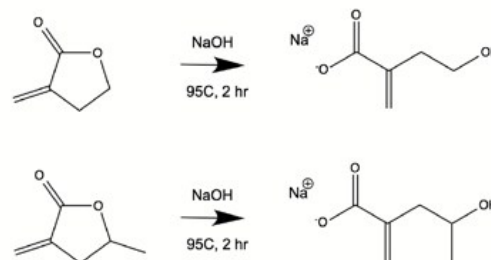
### Materials

The following chemicals were purchased from Sigma-Aldrich, Canada and used as received:  $\alpha$ -methylene- $\gamma$ -butyrolactone (MBL, 97%), acrylamide (AM, >98%), *N,N'*-methylenebis(acrylamide) (BIS, 99%), deuterated dimethyl sulfoxide (DMSO, 99.9% D), 2,2'-azobis(2-methylpropionamide) dihydrochloride (V-50 initiator, 97%), 4,4'-azobis(4-cyano-valeric acid) (ACVA initiator, >98%), potassium persulfate (KPS initiator, >99%), sodium hydroxide (NaOH, >97%). Deuterated water (D<sub>2</sub>O, 99.8% D) and hydrochloric acid (HCl, 36.5% w/w) were purchased from Fisher Scientific, Canada

and the  $\gamma$ -methyl- $\alpha$ -methylene- $\gamma$ -butyrolactone (MeMBL, >97%) was provided by DuPont Central Research Laboratories. Ultrapure water was obtained from Ultrapure Water System NW Series (Heal Force Bio-Meditech Holdings, Ltd., China). Lithium monoacylphosphine oxide (LiTPO), the photoinitiator used in the PLP-SEC experiments, was provided by Prof. Robert Liška's research group from Technische Universität Wien, Austria.

### Ring-opening saponification of MBL and MeMBL

The procedure for the ring-opening of MBL and MeMBL (Scheme 1) for *in-situ* NMR studies follows that previously developed for MBL.<sup>20</sup> For 1 g of MBL or MeMBL, 10 mol% excess of NaOH was measured and dissolved in 1 g of D<sub>2</sub>O in a 20 mL vial with a stir-bar. The saponification reaction took place in an oil bath at 95°C for 2 h, after which the solution was cooled to room temperature and 1 M HCl was added until a pH of 7 was reached. The SHMB or SHMeMB solution was then diluted with D<sub>2</sub>O to a final monomer concentration of 40 wt% (including mass of sodium ions). A similar procedure was done for the PLP-SEC and hydrogel studies, except that ultrapure water was used instead of deuterated water. The stock solution was mixed with other components to achieve desired concentrations for the *in-situ* NMR, PLP-SEC, or hydrogel studies. It should be mentioned that the influence of dilution and additional components on system pH was negligible. The structure of MeMBL was confirmed by NMR (Figure S1 of Supporting Information), and NMR was also used to confirm that the ring structure was completely opened to make SHMeMB (Figure S2).



Scheme 1: Ring-opening saponification of MBL to produce SHMB (top) and of MeMBL to produce SHMeMB (bottom) using 1.1 molar ratio of NaOH to butyrolactone ring at 95°C for 2 hours in water.

### Superabsorbent Hydrogel Synthesis and Characterization

Hydrogels were prepared using SHMeMB:AM molar ratios of 2:8, 4:6, and 6:4 (corresponding to  $f_{\text{SHMeMB}}$  of 0.2, 0.4 and 0.6, respectively), with 0.4 mol% of V-50, 1.0 or 1.5 mol% of BIS, and either 15 or 30 wt% monomer content in H<sub>2</sub>O. After purging with nitrogen for 10 min, the mixture was injected into a sealed glass cell that was held at 50°C for 16 h to yield a hydrogel of 1 mm in thickness and about 5 cm in width and length. A circular piece of hydrogel 13 mm in diameter was cut and immersed in ultrapure water at room temperature and water sorption was determined using an analytical balance. The swollen hydrogel was removed from solution, patted dry to remove excess water

and weighed at set intervals; fresh ultrapure water was added after each measurement. Measurements were less frequent for hydrogels that had lower mechanical strength in order to minimize breakage. It was assumed that this process leached all residual monomer from the hydrogel after 24 h, which was shown to be sufficient time for the swollen hydrogel to reach its equilibrium absorbency in the previous study.<sup>20</sup> The swollen samples were then freeze dried to remove the water and then weighed to determine the mass of the dried crosslinked polymer.

The gel yield ( $X_{\text{gel}}$ ) and swelling ratio (%) were calculated using Equation 1 and 2, respectively,

$$X_{\text{gel}} = \frac{m_{\text{dry}}}{m_{\text{initial}} w_{\text{M}}} \quad (1)$$

$$\text{Swelling Ratio [\%]} = \frac{m_{\text{wet}} - m_{\text{dry}}}{m_{\text{dry}}} \times 100\% \quad (2)$$

where  $m_{\text{initial}}$  and  $m_{\text{dry}}$  are the masses of as prepared hydrogel sample and sample after lyophilization, respectively,  $w_{\text{M}}$  is the weight fraction of monomers in the initial reaction mixture and  $m_{\text{wet}}$  is the mass of hydrogel sample measured at various time points during the swelling study.

Stress vs. strain curves of the swollen hydrogels were obtained at  $25 \pm 0.1^\circ\text{C}$  using an MCR-502 instrument (Anton Par, Austria) and Peltier accessories with a PP10 upper plate, with a solvent trap used to keep samples from dehydration. The mechanical tests were done in compression mode at a compression rate of  $0.6 \text{ mm}\cdot\text{s}^{-1}$ . Values shown in the plots were averaged from eight separate measurements. Storage and loss moduli measurements were also done with the same setup in the linear viscoelastic region, varying the frequency from 0.1 to 10 Hz. In addition, the swollen hydrogel samples were frozen with liquid nitrogen in order to obtain the cross section for scanning electron microscopy (SEM) imaging using a Nova NanoSEM instrument (FEI Quanta, Japan).

#### *In-situ* NMR studies

The *in-situ* NMR method was used to measure overall monomer conversion profiles, as well as the variation of monomer and polymer composition with conversion, following procedures described by Preusser and Hutchinson.<sup>21</sup> These studies were conducted without BIS crosslinker, over a range of SHMB:AM and SHMeMB:AM initial molar ratios and total monomer concentrations in  $\text{D}_2\text{O}$ , with the initiator content specified as weight percent of the total mixture (monomers +  $\text{D}_2\text{O}$ ).

Overall conversion  $X(t)$  was calculated from the decrease in monomer peak integrations relative to the HOD reference peak using Equation 3, where  $A_{\text{SHMeMB}}(0)$  and  $A_{\text{SHMeMB}}(t)$  are the areas of the SHMeMB proton peak at time = 0 and time =  $t$ , respectively, and  $A_{\text{AM}}(0)$  and  $A_{\text{AM}}(t)$  are the areas of the corresponding AM proton peaks. The proton peak assignments for SHMeMB and AM are shown in Figure S3. Individual conversions of SHMeMB and AM, calculated using Equation 4

and Equation 5, were used to calculate  $f_{\text{SHMeMB}}$ , the mole fraction of SHMeMB in the monomer mixture (Equation 6), with  $F_{\text{SHMeMB}}$ , the SHMeMB mole fraction in the copolymer, calculated from mass balance according to Equation 7.

$$X(t) = \frac{(A_{\text{SHMeMB}}(0) - A_{\text{SHMeMB}}(t)) + (A_{\text{AM}}(0) - A_{\text{AM}}(t))}{A_{\text{SHMeMB}}(0) + A_{\text{AM}}(0)} \quad (3)$$

$$X_{\text{SHMeMB}}(t) = \frac{A_{\text{SHMeMB}}(0) - A_{\text{SHMeMB}}(t)}{A_{\text{SHMeMB}}(0)} \quad (4)$$

$$X_{\text{AM}}(t) = \frac{A_{\text{AM}}(0) - A_{\text{AM}}(t)}{A_{\text{AM}}(0)} \quad (5)$$

$$f_{\text{SHMeMB}}(t) = \frac{A_{\text{SHMeMB}}(t)}{A_{\text{AM}}(t) + A_{\text{SHMeMB}}(t)} \quad (6)$$

$$F_{\text{SHMeMB}}(t) = \frac{X_{\text{SHMeMB}}(t)A_{\text{SHMeMB}}(0)}{X_{\text{SHMeMB}}(t)A_{\text{SHMeMB}}(0) + X_{\text{AM}}(t)A_{\text{AM}}(0)} \quad (7)$$

#### PLP-SEC studies

PLP experiments were performed using an excimer laser (ExciStar XS 500, Coherent, Inc.) operated at 351 nm with corona preionization and an all-solid-state-pulsar. Pulse repetition rate was varied between 1-5 Hz with 3 mJ of laser energy per pulse. Appropriate molar ratios of monomers in ultrapure water with LiTPO photoinitiator were prepared. Reaction mixtures of 1 mL were placed in 110 OS cells (Hellma GmbH & Co. KG, Germany) with a path length of 10 mm. Prior to PLP, cells were purged with nitrogen for 2 min and sealed with a PTFE stopper, then heated for 20 min up to reaction temperature. The reaction mixtures were kept in a dark area to avoid initiation of polymerization prior to the laser pulsing. A beam expander BXUV-10.0-3X (CVI Melles Griot, USA) was placed between the laser and the cell to evenly distribute the laser beam throughout the cell. After the PLP, polymer solutions were transferred into vials containing small amounts of hydroquinone monomethyl ether to inhibit post-polymerization. Polymer solutions were transferred into 3500  $\text{g}\cdot\text{mol}^{-1}$  dialysis tubes (Spectra/Por 6, Spectrum Laboratories, Inc., Compton, CA) in ultrapure water for 3 days (with frequent changes of water), then freeze-dried using a Mini-Lyotrap (LTE Scientific, Greenfield, UK).

Polymer molar mass analysis was performed using a Waters size-exclusion chromatograph with pump 515, an autosampler 717, a column heater, and 2414 refractive index detector. Polymer samples ( $1\text{-}2 \text{ mg}\cdot\text{mL}^{-1}$ ) were dissolved in eluent ( $0.1 \text{ mol}\cdot\text{L}^{-1} \text{ Na}_2\text{HPO}_4$  and 100 ppm  $\text{Na}_3\text{N}$ ) with added ethylene glycol as flow marker, and stirred for 24-48 h. The aqueous polymer solutions were filtered using  $0.45 \mu\text{m}$  nylon membrane filters (Millex-HN, Millipore, Ireland) before being injected into the system with a flow rate of  $0.5 \text{ mL}\cdot\text{min}^{-1}$ . The columns setup (Polymer Standards Service, Mainz, Germany) consisted of an  $8 \times 50 \text{ mm}$  guard Suprema column, and three  $8 \times 300 \text{ mm}$  Suprema columns with  $10 \mu\text{m}$  particle size and pore sizes of 100, 1000, and  $3000 \text{ \AA}$  maintained at  $60^\circ\text{C}$ . Polyacrylamide standards

(American Polymer Standards Corp.) with peak molar masses between 2950 and 950 000 g·mol<sup>-1</sup> were used for calibration, with data analysis done using PSS WinGPC Unichrom software. Polymer molar mass values are reported relative to polyacrylamide standards, however, they can be considered as reasonably accurate, since the AM-rich copolymers contained only 5-15 mol% of SHMeMB or SHMB.

## Results and Discussion

### Ring-closure of SHMB and SHMeMB

Before proceeding with hydrogel formation and *in-situ* NMR studies, it was necessary to verify that SHMeMB does not undergo side reactions under synthesis conditions. In the previous study there was evidence of SHMB ring-closure to form MBL during homopolymerization: insoluble polymer was observed after 16 h polymerization of 30 wt% SHMB monomer with 0.2 mol% ACVA at 75°C and a pH of 7, and 4 mol% of the monomer remaining in solution was determined by NMR to be MBL rather than SHMB.<sup>20</sup> As the MBL amount increased as pH was lowered, it was concluded that the ring-closure was catalyzed in acidic conditions, and that the resulting precipitate was evidence of poly(MBL), which is insoluble in water. The study also found that homopolymerization of SHMB in water was very slow,<sup>20</sup> especially relative to rates of radical polymerization of MBL in organic solution.<sup>17</sup> As it is well known that values of  $k_p$  in water are significantly higher than in organic solution (for example, as seen for methacrylic acid<sup>28</sup>), it is likely that MBL formed from ring-closure of SHMB was quickly polymerized to form poly(MBL).

Similar experiments were done in this study to determine if ring-closure of SHMeMB to form MeMBL occurred. Homopolymerizations were conducted at pH=7 with both V-50 and ACVA initiators at 15 wt% monomer and 50 and 75°C. There was no evidence of MeMBL monomer peaks observed in the NMR spectra after a reaction time of 16 h, and no polymer precipitate was observed. Thus, it can be concluded that, contrary to SHMB homopolymerization with ACVA, SHMeMB did not undergo ring-closure. Further investigations found that polymer precipitate was observed under more acidic conditions, i.e., with pH decreased to 4 and 5 using 1 M HCl and homopolymerizations conducted at both 50 (1 wt% V-50) and

75°C (1 wt% KPS) for 16 h; the amount of precipitate increased at lower pH and higher temperature. NMR was used to verify this trend; as shown in Figure S4 and Figure S5, the amount of MeMBL dissolved in the aqueous phase at the end of the 16 h reaction at 75°C was less than 3 mol% at pH=5 and about 9 mol% at pH=4. While the cause of the differences between the two monomers is not certain it can be concluded that ring-closure of both SHMB and SHMeMB does not occur if pH is equal or greater than 7 at 55°C, conditions maintained throughout the remainder of this study.

### Superabsorbent hydrogel absorption

Superabsorbent hydrogels were synthesized by copolymerizing SHMeMB and AM with small amounts of BIS crosslinker at varying molar ratios of SHMeMB:AM, similar to conditions used to produce SHMB:AM hydrogels in the study of Kollár *et al.* [20]. The initial reactions were conducted with solutions containing 0.2 mol% V-50 and 15 wt% monomer in water at 50°C for 4 h. The resulting hydrogels, however, lacked mechanical strength (i.e., very soft and jelly like, difficult to handle), with a significant amount of unreacted monomer remaining in solution, unlike found for SHMB:AM hydrogels made at the same conditions. It was also observed qualitatively that the fragility of the swollen hydrogels increased as the SHMeMB content was increased from 20 to 60 mol% in the formulations.

The increased fragility of SHMeMB:AM relative to SHMB:AM hydrogels was contrary to the expectation that the fragility would decrease with the bulkier side group in the polymer chain. In a study regarding properties of (meth)acrylate crosslinked polymers, it was found that both the length of the ester side group and the addition of the  $\alpha$ -methyl side group increased  $T_g$ .<sup>29</sup> Nonetheless, the increasing mechanical strength found with increasing AM is consistent with the relative properties of crosslinked poly(AM) and poly(sodium acrylate) homopolymers:<sup>30</sup> poly(AM) has a higher shear modulus, and poly(sodium acrylate) chains are more extended due to repulsion of the charged moieties. Increasing the initial monomer concentration during synthesis is also known to affect properties of the crosslinked polymer, as chain transfer to polymer is more likely to occur with increased conversion, giving rise to branching and self-crosslinking, and therefore

Table 1: Total monomer ( $M$ ) conversions of SHMB:AM copolymerizations conducted with 15 wt% initial monomer<sup>20</sup> and SHMeMB:AM copolymerizations with 15 and 30 wt% initial monomer in aqueous solutions at varying feed molar fractions of SHMB ( $f_{SHMB}$ ) and SHMeMB ( $f_{SHMeMB}$ ) at 50°C.

$f_{SHMB}$	0.2		0.4		0.6	
V-50 mol%	0.2	-	0.2	-	0.2	-
M/H <sub>2</sub> O wt./wt.	15/85	-	15/85	-	15/85	-
Reaction time (hrs)	4	-	4	-	4	-
Conversion	97%	-	92%	-	59%	-
$f_{SHMeMB}$	0.2		0.4		0.6	
V-50 mol%	0.2	0.2	0.4	0.2	0.2	0.4
M/H <sub>2</sub> O wt./wt.	15/85	30/70	30/70	15/85	30/70	30/70
Reaction time (h)	16	16	16	16	16	16
Conversion	72%	84%	97%	44%	50%	66%
				35%	40%	44%

hydrogels of higher rigidity.<sup>31</sup> Thus, the monomer concentration in this study was increased from 15 wt% to 30 wt% and reaction time from 4 to 16 h in order to achieve a sufficient conversion and more stable hydrogel for subsequent swelling experiments.

To better understand these results, the experiments were repeated in D<sub>2</sub>O solution without crosslinker in order to determine the final monomer conversion using NMR and to compare to results for SHMB:AM copolymerization reported by Kollár *et al.*<sup>20</sup> As shown in Table 1, conversion decreased with decreasing AM content for both systems, indicating that both SHMB and SHMeMB slow the overall rate of copolymerization. SHMeMB:AM copolymers reached a lower conversion than SHMB:AM for all 3 molar ratios. The conversion of the system increased slightly when monomer content was increased from 15 to 30 wt% at identical initiator loading, consistent with previous studies showing an increase in  $k_p$  values for methacrylic acid<sup>26</sup> with monomer concentration.

Increasing reaction time, increased initiator levels and overall monomer concentration provide sufficient conversion for subsequent testing of hydrogels. The swelling experiments and determination of mechanical properties were performed on hydrogels synthesized with 0.4 mol% of V-50 for 16 h at 30 wt% monomer concentration. Conversions of monomer to gel (gel yield), calculated from weight of the dry hydrogel using Equation 1 were in quite good agreement with the conversions estimated by NMR from copolymerizations performed in D<sub>2</sub>O without addition of crosslinker (Table 2).

Table 2: Individual comonomer conversions ( $X_{AM}$  and  $X_{SHMeMB}$ ) molar fractions of monomers incorporated into the final polymer ( $F_{AM}$  and  $F_{SHMeMB}$ ) total monomer conversion ( $x$ ) calculated from <sup>1</sup>H NMR for linear polymers, and yield of crosslinked polymer ( $X_{gel}$ ) based on gravimetric analysis of crosslinked polymers prepared with various feed molar fractions of monomers,  $f_{AM}$  and  $f_{SHMeMB}$ .

$f_{AM} / f_{SHMeMB}$	$F_{AM} / F_{SHMeMB}$	$X_{AM}$ (%)	$X_{SHMeMB}$ (%)	$x$ (%)	$X_{gel}$ (%)
0.80 / 0.20	0.81 / 0.19	98	89	97	90±2
0.60 / 0.40	0.71 / 0.29	78	48	66	61±2
0.40 / 0.60	0.60 / 0.40	66	29	44	54±1

As shown in Figure 1 for material synthesized with 1.5 mol% crosslinker and  $f_{SHMeMB} = 0.2$  as an example, the hydrogels swell significantly from their original size of 1 mm in thickness and 13 mm in diameter during the swelling studies. After 24 h, swelling of the hydrogels was assumed to have reached equilibrium (Figure 1a).

The water absorption of the complete set of SHMeMB:AM hydrogels is compared in Figure 2. With 1.0 mol% crosslinker, swelling ratios of  $f_{SHMeMB} = 0.6$  and 0.4 samples were 59,000% and 33,000%, respectively. These values were higher than values found for the corresponding SHMB:AM hydrogels (40,000% and 20,000% for  $f_{SHMB} = 0.6$  and 0.4, respectively<sup>20</sup>). Interestingly, the lowest content of SHMeMB in hydrogel ( $f_{SHMeMB} = 0.2$ ) results in lower water absorption compared to

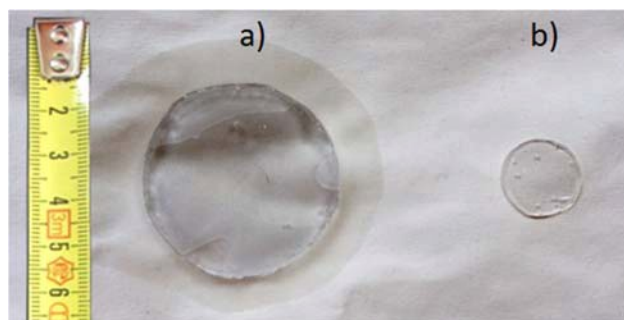


Figure 1: SHMeMB:AM hydrogel ( $f_{SHMeMB} = 0.2$ ) with 1.5 mol% crosslinker after swelling (a) and before, i.e. as prepared (b).

the corresponding SHMB hydrogel (8,600% vs 13,000%). It should be pointed out, however, that direct comparison of SHMeMB:AM and SHMB:AM hydrogels is not strictly valid, since they differ in the monomer and initiator contents used during preparation due to the lower SHMeMB:AM reactivity. The higher monomer and initiator content should provide a denser network at similar monomer conversion, which could lead to the lower water absorption observed for  $f_{SHMeMB} = 0.2$ . However, the lower monomer conversions obtained with  $f_{SHMeMB} = 0.4$  and 0.6 (compared to SHMB) likely lead to lower network densities, providing the higher water absorption observed. Nonetheless, the trend of higher absorbency with increased SHMeMB content is consistent with the results reported for SHMB:AM and conventional poly(sodium acrylate-co-acrylamide) hydrogels, as the carboxylate groups are more hydrophilic than the acrylamide groups.<sup>32</sup> In addition, the crosslinked network becomes more expanded due to electrostatic repulsion of the ionized groups, with the SHMeMB unit providing more hydrophilicity to these hydrogels than

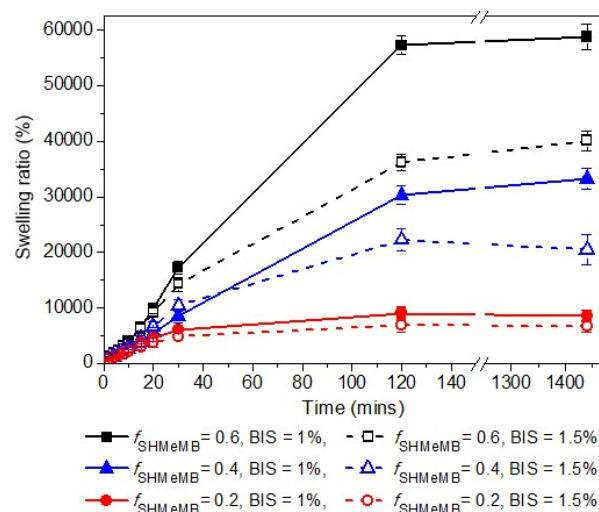


Figure 2: Swelling ratios of AM:SHMeMB hydrogels made with 0.4 mol% V-50 at 30 wt% monomer for 16 h at varying initial comonomer ratios and BIS crosslinker content (mol%), as indicated.

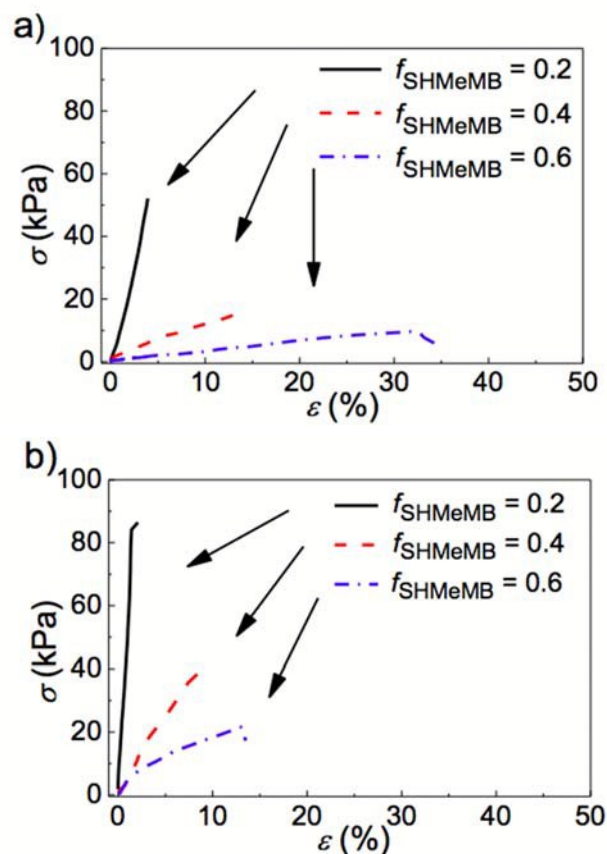


Figure 3: Stress vs. strain curves of hydrogels made with a) 1.0 mol% BIS and b) 1.5 mol% BIS and initial comonomer molar ratios of  $f_{\text{SHMeMB}} = 0.2, 0.4$  and  $0.6$  with 30 wt% monomer and 0.4 mol% V-50 in aqueous solution for 16 h at 50°C.

sodium acrylate. Increasing the crosslinker concentration from 1 mol% to 1.5 mol% showed the expected behaviour, with a slight decrease of swelling ratios measured for all samples (Figure 2).

The mechanical strength of the hydrogels was quantified from the stress vs. strain curves obtained under compression, as shown in Figure 3. Hydrogels with increased AM content were able to withstand higher compression stress, indicating a higher mechanical strength. In addition, higher compression stress was observed for hydrogels prepared with higher cross-linker concentration.

Storage ( $G'$ ) and loss ( $G''$ ) moduli are shown as a function of frequency in Figure 4. The storage modulus is constant with frequency, consistent with the expected properties of cross-linked viscoelastic materials.  $G'$  increased from 680 to 13100 Pa with increasing AM content in the hydrogels synthesized with 1.0 mol% of BIS, and from 1200 Pa to 32000 Pa with 1.5 mol% of BIS, indicating that AM provides mechanical strength of the hydrogels. Similarly to the  $G'$  behaviour,  $G''$  is also nearly independent of the frequency, indicating that the hydrogels were well cross-linked, with relatively low energy dissipation observed especially at higher AM contents. Overall, the

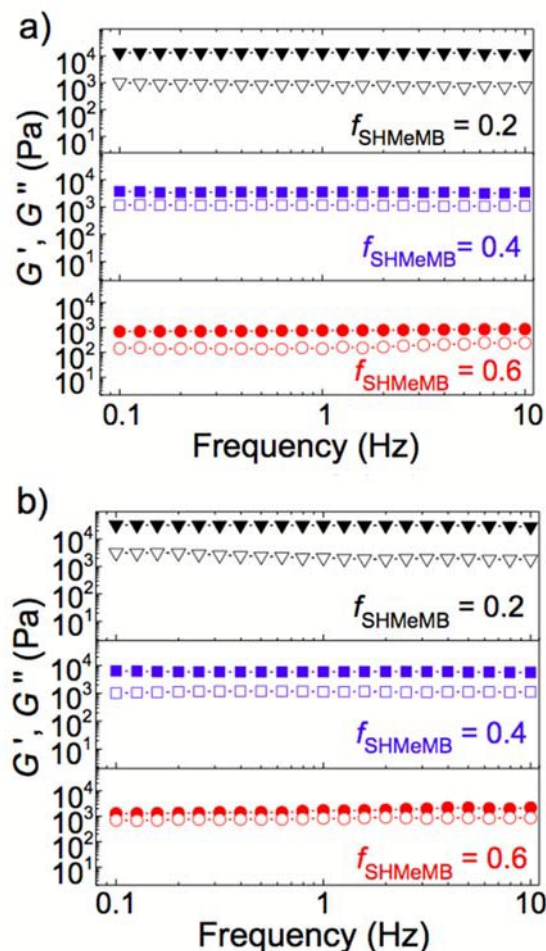


Figure 4: Storage ( $G'$ , filled symbols) and loss ( $G''$ , open symbols) moduli measured as a function of frequency for SHMeMB:AM hydrogels produced with monomer molar ratios of  $f_{\text{SHMeMB}} = 0.2$  (top),  $0.4$  (middle) and  $0.6$  (bottom) with a) 1.0 and b) 1.5 mol% of BIS.

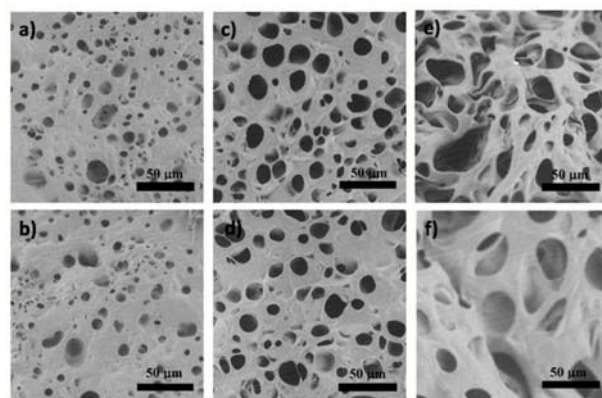


Figure 5: SEM images of freeze-dried cross-sections of the SHMeMB:AM hydrogels synthesized at a molar ratio of  $f_{\text{SHMeMB}} = 0.2$  with a) 1.0 mol% and b) 1.5 mol% BIS; a molar ratio of  $f_{\text{SHMeMB}} = 0.4$  with c) 1.0 mol% and d) 1.5 mol% BIS; and a molar ratio of  $f_{\text{SHMeMB}} = 0.6$  with e) 1.0 mol% and f) 1.5 mol% BIS. Hydrogels were synthesized from 30 wt% monomer and 0.4 mol% V-50 for 16 h at 50°C.

mechanical properties of SHMeMB:AM hydrogels are highly-tunable and can be tailored by changing the amount of crosslinker and the molar composition of the copolymer. The hydrogels of higher AM content, having better mechanical properties, could be suitable for a variety of applications such as cell culturing or tissue engineering,<sup>33</sup> while those produced with higher SHMeMB content exhibit promise as superabsorbent materials.

SEM images shown in Figure 5 indicate that the porosity of the hydrogels is higher with increasing amount of SHMeMB. Porosity decreased at higher crosslinker level, indicating the formation of a denser polymer network consistent with the degree of swelling results. SEM images of poly(sodium acrylate – co – acrylamide)/graphene oxide hydrogels also indicated a smoother polymer surface and a denser hydrogel with increasing crosslinker content.<sup>34</sup>

### Kinetic Studies using *in-situ* NMR

The decrease in total monomer conversion with increasing SHMeMB content is due to the lower reactivity of SHMeMB, slowing both the overall copolymerization rate and the relative rate of SHMeMB incorporation into the copolymer. Due to the significant difference in reactivity compared to the SHMB:AM system, further kinetic studies were done to better understand and quantify the influence of SHMeMB on the copolymerization system.

Using the *in-situ* NMR method, the consumption of the individual monomers can be monitored by following the change in their proton peak intensities with reaction time, providing both a continuous measure of overall monomer conversion, as well as the change in comonomer (and thus copolymer) composition over the course of the batch reaction. In Figure 6, the increases in overall monomer conversion of SHMeMB:AM and SHMB:AM systems under identical conditions are shown for both 2:8 and 4:6 initial molar ratios. It is evident that SHMB:AM copolymers have a faster rate of polymerization, in agreement with the observations made during hydrogel synthesis. A

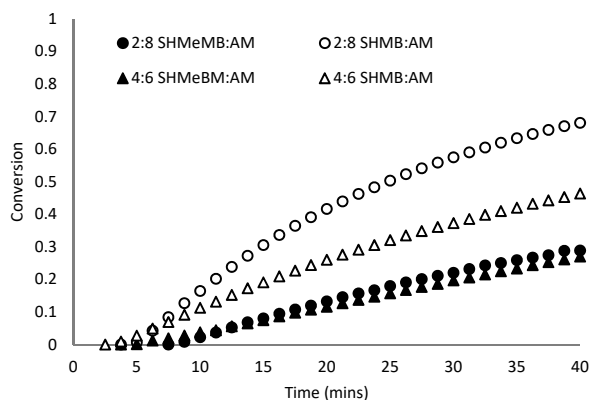


Figure 6: Overall monomer conversion profiles for polymerization of  $f_{\text{SHMeMB}} = 0.2$  and  $f_{\text{SHMeMB}} = 0.4$  initial molar ratios of SHMeMB:AM and SHMB:AM at 50°C with 15 wt% monomer and 0.5 wt% V-50 initiator in  $\text{D}_2\text{O}$ .

comparison of these plots indicates that the rate of monomer conversion decreases for both systems as the initial AM fraction is decreased.

A series of SHMeMB:AM copolymerizations at various molar ratios were completed at 50°C with 0.5 wt% V-50 and 15 wt% monomer. The drift in monomer composition (molar fraction SHMeMB, denoted by  $f_{\text{SHMeMB}}(t)$ ) with conversion is shown in Figure 7. Despite the lowering of polymerization rate observed with increasing SHMeMB level, there is only a slight drift in  $f_{\text{SHMeMB}}(t)$  with conversion, with the increasing value indicating preferential incorporation of AM into the copolymer. Material balances were used to calculate the composition of the copolymer formed at low (<10%) conversion, with results summarized in Table S4. The low-conversion data was used to construct a Mayo-Lewis plot to represent the relationship between comonomer and copolymer composition, as shown in Figure 8a. Also included on the plot is the previously reported fit for SHMB:AM data fit to the terminal model resulting in reactivity ratios  $r_{\text{SHMB}}=0.35\pm0.15$  and  $r_{\text{AM}}=1.42\pm0.40$ .<sup>20</sup> From this study the reactivity ratios for SHMeMB:AM were determined to be  $r_{\text{SHMeMB}}=0.12\pm0.08$  and  $r_{\text{AM}}=1.10\pm0.01$ . The two sets of data overlap below a comonomer fraction of 0.4, but the incorporation of SHMeMB is lowered at higher comonomer levels, leading to the significant difference in the reactivity ratio estimates.

As shown in previous work, more precise estimates of reactivity ratios can be obtained by fitting an integrated form of the Mayo-Lewis equation to the drift in monomer composition as a function of conversion.<sup>21</sup> Figure 7 demonstrates that the best-fit values of  $r_{\text{SHMeMB}}=0.17\pm0.01$  and  $r_{\text{AM}}=0.95\pm0.01$  estimated using the entire set of composition drift data provide an excellent representation of the *in-situ* NMR results. While there is a minor difference between the estimates, both the values determined using the entire monomer composition drift and those fit to the low-conversion data provide a similar

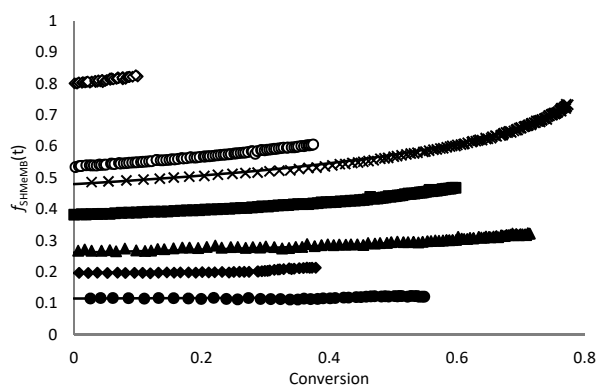


Figure 7: SHMeMB monomer content ( $f_{\text{SHMeMB}}(t)$ ) as a function of conversion at varying feed molar ratios of SHMeMB:AM ( $f_{\text{SHMeMB}}$  values between 0.1 and 0.8) at 15 wt% monomer and 0.5 wt% V-50 at 50°C. Lines represent monomer composition drift computed using the integrated form of the Mayo-Lewis equation with best fit reactivity ratios of  $r_{\text{SHMeMB}}=0.17$  and  $r_{\text{AM}}=0.95$ .



ARTICLE

Journal Name

representation of copolymer vs comonomer composition, as evidenced by comparing the two curves generated in Figure 8b. Although there is no discernable difference in addition rates of AM and SHMeMB monomer to an AM macroradical ( $r_{AM} \approx 1$ ), there is a clear preference for AM monomer to add to the anionic SHMeMB radical compared to SHMeMB monomer addition. A comparison of the two systems indicates there is a lower tendency for SHMeMB to homopolymerize compared to SHMB, most likely due to the presence of the extra methyl group (see Scheme 1).

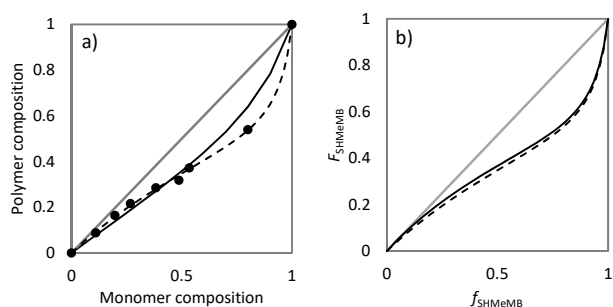


Figure 8: (a) Mayo-Lewis curves for SHMB:AM<sup>20</sup> (solid line) and SHMeMB:AM (points are experimental data and dashed line is best-fit curve) radical copolymerization at 15 wt% monomer and 50°C, where the x-axis represents SHMB (or SHMeMB) molar fraction in the monomer mixture and the y-axis represents the SHMB (or SHMeMB) molar fraction in the copolymer at low conversion. (b) Mayo-Lewis curves for SHMeMB:AM copolymerization calculated using best-fit reactivity ratios estimated from both low conversion data (dashed line,  $r_{SHMeMB}=0.12$  and  $r_{AM}=1.10$ ) and the integrated form of the Mayo-Lewis equation (solid line,  $r_{SHMeMB}=0.17$  and  $r_{AM}=0.95$ ).

PLP-SEC kinetic studies

To further investigate the difference in reactivity between SHMB:AM and SHMeMB:AM copolymers, PLP-SEC studies were done to determine propagation rate coefficients. In this technique, observable features on the polymer molar mass distribution (MMD) correlate to the time between two consecutive laser pulses, as initiation of radicals in the system is controlled by activation of the photoinitiator by the laser.<sup>22</sup> The first pulse generates a radical population which continues to propagate (and terminate) in the subsequent “dark” period. The second pulse generates a new radical population that increases the likelihood of chain termination of those radicals that have survived to that point, with the burst of termination producing an increased population of dead polymer chains observable in the resultant polymer MMD. Chains that are not terminated by the consecutive pulse will continue to propagate such that the increased probability of termination that occurs at the next pulse also creates an observable a second peak (or shoulder) in the MMD. PLP-SEC is an accurate technique in determining  $k_p$  with little scatter, with the estimates found to be independent of chain length, initiator concentration, or repetition rate for methyl methacrylate,<sup>35</sup> styrene,<sup>22</sup> and butyl acrylate.<sup>36</sup> As discussed in these references, the inflection points associated with the MMD features are used to determine  $k_p$  using Equation (8);  $L_1$  represents the polymer molar mass at the first inflection point (determined from the position of the maximum of the first-derivative of the distribution) associated with chain growth between two consecutive laser pulses, and  $L_2, L_3, \dots$  are higher

order inflection points for polymer chains that have a lifetime of ( $i \cdot t_0$ ). Monomer concentration,  $c_M$ , is assumed to be constant as polymer conversion is kept very low and the time between pulses,  $t_0$ , is the reciprocal of the laser pulse repetition rate.

$$L_i = i k_p c_M t_0 \quad i = 1, 2, 3, \dots \quad (8)$$

The technique can also be robustly applied to comonomer mixtures, where the resulting estimate of  $k_p$  represents the composition-averaged copolymerization propagation rate coefficient,  $k_p^{cop}$ .

Previous experiments for AM homopolymerization in aqueous solution at 10 wt% and at 60 °C resulted in good PLP structures at pulse repetition rates of 150 and 300 Hz and 100 and 300 pulses; the resulting  $k_p$  value under these conditions was  $110\,000\text{ L}\cdot\text{mol}^{-1}\cdot\text{s}^{-1}$ .<sup>27</sup> Thus, the first PLP-SEC experiments for SHMeMB:AM were done under similar conditions, the only difference being 10 mol% SHMeMB introduced, with total monomer content in water remaining at 10 wt%. Laser frequency was varied between 5 and 300 Hz, and a significantly larger number of pulses (1000 or 1500) was used with  $3.4\text{ mmol}\cdot\text{L}^{-1}$  LiTPO. As the hydrogel synthesis demonstrated that

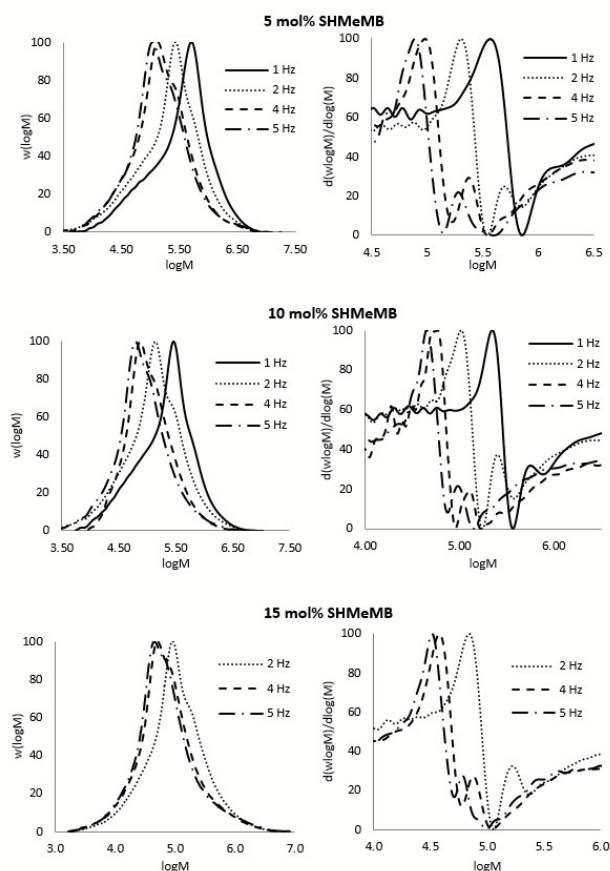


Figure 9: Polymer molar mass distributions (left) and first derivative plots (right) produced by PLP of SHMeMB:AM mixtures of varying compositions at 10 wt% monomer,  $6.8\text{ mmol}\cdot\text{L}^{-1}$  LiTPO, and 60°C. PLP-SEC experiments for  $f_{SHMeMB}=0.10$  were done with number of pulses=100, and  $f_{SHMeMB}=0.05$  and  $0.15$  were done with number of pulses=50.

SHMeMB is much less reactive than AM, the lower frequencies were used to allow for a longer dark period, with the higher number of pulses to increase conversion. However, these PLP conditions did not lead to well-structured MMDs (Figure S6 and Figure S7), as there was no evidence of multiple inflections to accurately determine  $k_p^{\text{cop}}$ .

Thus, a new set of PLP experiments was done with the pulse repetition rate lowered to between 1 and 5 Hz with 6.8 mmol·L<sup>-1</sup> LiTPO, and the number of pulses reduced to 50 and 100 in order to improve the features of the distributions. SHMeMB:AM mixtures of 10 wt% total monomer in water were examined, with 5, 10, and 15 mol% of SHMeMB. The resulting polymer MMDs and their first derivative plots (used to identify the points of inflection  $L_i$ ) are shown in Figure 9. In most of the cases, there is more than one inflection point, indicating that the experiments can be used to determine  $k_p^{\text{cop}}$ . As mentioned in the Experimental Methods section, MMDs were analyzed using PAM calibration, although the copolymers contained up to 15 mol% SHMeMB.

In order to verify the accuracy of the  $k_p^{\text{cop}}$  values calculated from these PLP structures, the ratio of molecular weights at the first

and second inflection points were determined ( $L_1/L_2$ ). In some cases, the experimental ratios were slightly below the expected value of 0.5, perhaps due to the higher conversion of some experiments, as the decreased monomer concentration can cause small shifts in the distribution. Thus, the conversion was reduced to <10% by lowering the number of pulses from 100 to 50 in later experiments. Due to the limited number of successful experiments, all values were used to estimate  $k_p^{\text{cop}}$ , as the values determined from experiments at different pulse repetition rates are in good agreement as seen by inspecting the full set of data in Table S5.

The same PLP conditions were used for SHMB:AM to produce a direct comparison of  $k_p^{\text{cop}}$  for the two systems. Their MMDs and first derivative plots are shown in Figure 10 for 5-15 mol% of SHMB in SHMB:AM mixtures of 10 wt%, with full results summarized in Table S6. For the SHMB copolymer system it was the experiments at higher pulse repetition rates of 4 and 5 Hz that yielded more distinct PLP-structured MMDs, unlike the 1 and 2 Hz required for SHMeMB:AM system at the same conditions. With SHMB:AM, the MMDs were broadened at lowered repetition rates, perhaps due to a higher termination rate in the system.

The  $k_p^{\text{cop}}$  values of SHMeMB:AM and SHMB:AM determined by PLP-SEC are compared in Figure 11, plotted as a function of molar fraction of AM and also as a function of comonomer molar fraction. For both systems,  $k_p^{\text{cop}}$  decreases rapidly when the comonomer is added to the AM system. Even 5 mol% of comonomer reduces  $k_p$  from the known homopolymerization value of 110 000 L·mol<sup>-1</sup>·s<sup>-1</sup> for AM<sup>27</sup> to 10 000 L·mol<sup>-1</sup>·s<sup>-1</sup> with 5 mol% SHMB and 4 300 L·mol<sup>-1</sup>·s<sup>-1</sup> with 5 mol% SHMeMB. These results also show that the SHMB:AM system is more reactive than SHMeMB:AM by greater than a factor of two.

PLP structures were not obtained for SHMB or SHMeMB homopolymers (or copolymers where  $f_{\text{SHMB}}$  and  $f_{\text{SHMeMB}}$  contents were higher than 15 mol%), as propagation for the

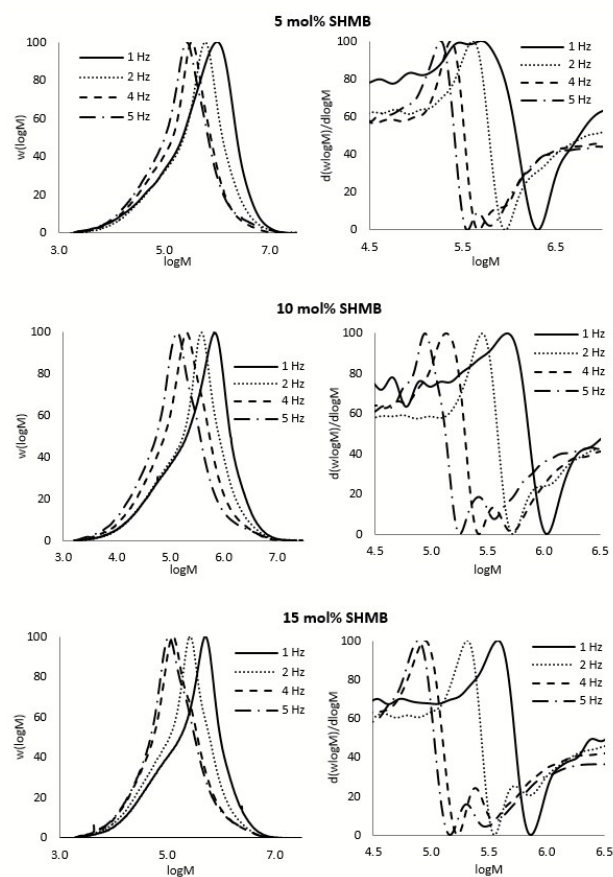


Figure 10: Polymer molar mass distributions (left) and corresponding first derivative plots (right) produced by PLP of SHMB:AM mixtures of varying compositions with number of pulses=50, 10 wt% monomer, 6.8 mmol·L<sup>-1</sup> LiTPO, and at 60°C.

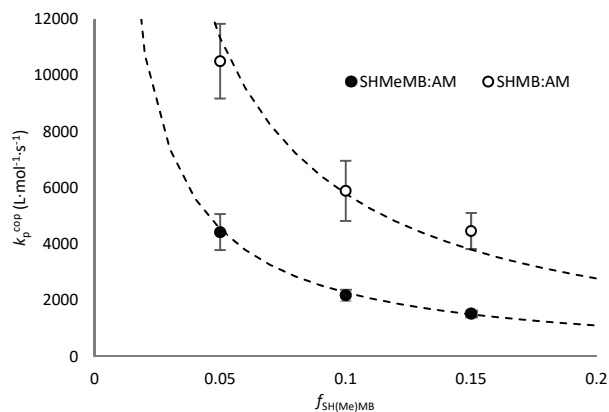


Figure 11:  $k_p^{\text{cop}}$  of SHMeMB:AM and SHMB:AM at varying molar ratios at 10 wt% monomer, 60°C and 6.8 mmol·L<sup>-1</sup> LiTPO with error bars representing standard deviation of the data set. The dashed line represents the terminal model estimating  $k_p^{\text{cop}}$  for all molar compositions of SHMB:AM and SHMeMB:AM.

homo/copolymerizations became too slow. Repetition rate of the laser pulse could not be decreased further to obtain characteristic MMD inflection points. However, assuming the terminal model,  $k_p$  of SHMB and SHMeMB homopolymers were estimated using Equation (9) to fit the variation in  $k_p^{\text{cop}}$  as a function of monomer composition ( $f_A$  and  $f_B = 1 - f_A$ , with  $A$  representing AM and  $B$  the SHMB or SHMeMB comonomer) using the determined monomer reactivity ratios ( $r_A$  and  $r_B$ ), monomer fractions and homopolymer  $k_p$  values.

$$k_p^{\text{cop}} = \frac{r_A f_A^2 + 2f_A f_B + r_B f_B^2}{\frac{r_A f_A}{k_{p,AA}} + \frac{r_B f_B}{k_{p,BB}}} \quad (9)$$

Using the known reactivity ratios of  $r_{\text{SHMB}}$  and  $r_{\text{AM}}$  from Kollár *et al* study [20],  $r_{\text{SHMeMB}}$  and  $r_{\text{AM}}$  from this study, and  $k_{p,AM}$  of 110 000 L·mol<sup>-1</sup>·s<sup>-1</sup> [27], the  $k_p$  values of SHMB and SHMeMB were estimated to be 165 and 25 L·mol<sup>-1</sup>·s<sup>-1</sup>, respectively, at 60°C. While these absolute values have significant uncertainty due to the limited number of data points, the extrapolation of the curve to  $f_{\text{SH(Me)MB}} = 1$ , and the assumption that the terminal model adequately describes the copolymerization propagation behavior, the PLP-SEC study indicates clearly that SHMB is more reactive than SHMeMB.

## Conclusions

MeMBL was successfully saponified to form a water-soluble SHMeMB monomer that does not undergo ring-closure at pH of 7 or greater. The synthesis of lightly crosslinked SHMeMB:AM hydrogels represents a unique approach for the preparation of superabsorbent material. The hydrogels attained equilibrium degree of swelling in the range of 6 700 – 59 000 %, depending on copolymer composition as well as crosslink density, with the swelling capacity significantly increasing with SHMeMB content. The monomer ratio and crosslinker concentration also influenced the porosity and overall mechanical properties of the hydrogels. These characteristics were shown to be highly tunable, allowing the potential to prepare tailored hydrogels with a wide range of potential applications.

Kinetic studies of SHMeMB:AM and SHMB:AM aqueous-phase radical copolymerization were conducted to investigate their reactivities using in-situ NMR and PLP-SEC techniques. The *in-situ* NMR studies revealed that SHMeMB:AM mixtures polymerized at slower rates than SHMB:AM, with comonomer composition drifts used to estimate the monomer reactivity ratios as  $r_{\text{SHMeMB}} = 0.12 - 0.17$  and  $r_{\text{AM}} = 0.95 - 1.10$ . The relative incorporation rate of SHMeMB into the copolymer was lower than that of SHMB for comonomer-rich mixtures. Using PLP-SEC, values for  $k_p^{\text{cop}}$  of SHMeMB:AM were shown to be lower than those of SHMB:AM. The data obtained at high AM content were fit by the terminal model to provide first estimates of the SHMeMB and SHMB homopropagation rate coefficients, albeit with high uncertainty. It is clear from the study, however, that the  $k_p$  value for SHMeMB is lower than that for SHMB, with both

values much lower, by three orders of magnitude, than the  $k_p$  of AM, explaining the long polymerization times required to synthesize the hydrogels. The lower reactivity of SHMeMB compared to SHMB in copolymerization with AM results in differing compositions and physical properties of the final hydrogels prepared with the same initial comonomer feed ratio. However, the overall properties of the hydrogels can still be easily tuned. As a more promising route has been developed for the production of SHMeMB from bio-sourced feedstock, further studies are underway to explore the homo- and copolymerization kinetics of SHMeMB:AM at different temperatures and monomer concentrations and with added salt, to further optimize the conditions for hydrogel synthesis.

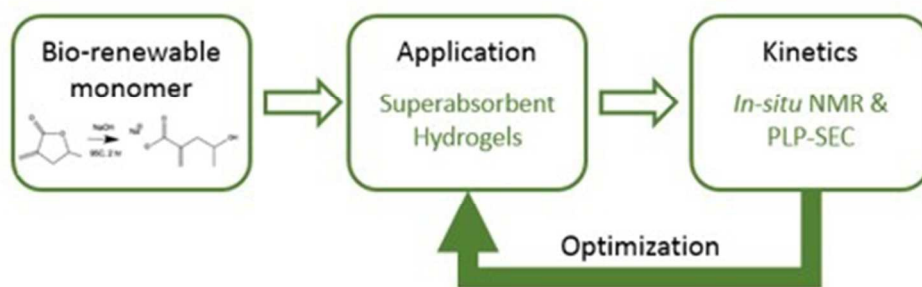
## Acknowledgements

Authors would like to thank European Regional Development Fund through project POLYFRIEND, project no. HUSK 1101/1.2.1/0209, within Hungary-Slovakia Cross-border Co-operation Programme 2007-2013 as well as to project VEGA 2/0158/17, Slovak Academic Information Agency (SAIA) for the National Scholarship Programme of the Slovak Republic, and Natural Sciences and Engineering Research Council of Canada (NSERC) for their financial support.

## Notes and references

- V. Kadajji, G. Betageri, *Polymers*, 2001, **3**, 1972-2009.
- D. Vedoy, J. Soares, *Can. J. Chem. Eng.*, 2015, **93**, 888-904.
- B. Rivas, E. Pereira, M. Palencia, J. Sánchez, *Prog. Polym. Sci.*, 2011, **36**, 294-322.
- U. B. Nurmatov, N. Tagiyeva, S. Semple, G. Devereux and A. Sheikh, *Eur. Respir. Rev.*, 2015, **24**, 92-101.
- J. P. Dawson, B. J. Bloomer, D. A. Winner and C. P. Weaver, *Bull. Amer. Meteor.*, 2014, 521-532.
- B. Nimana, C. Canter and A. Kumar, *Appl. Energy*, 2015, **143**, 189-199.
- P. Cashin, K. Mohaddes, M. Raissi and M. Raissi, *Energ. Econ.*, 2014, **44**, 113-134.
- R. Auras, L. T. Lim, S. E. Selke and H. Tsuji, *Poly(lactic acid): Synthesis, Structures, Properties, Processing, and Applications*, John Wiley & Sons, 2010.
- K. Sudesh, H. Abe and Y. Doi, *Prog. Polym. Sci.*, 2000, **25**, 1503-1555.
- J. Zhao and H. Schlaad, *Adv. Polym. Sci.*, 2013, **253**, 151-190.
- Y. Kato, H. Yoshida, K. Shoji, Y. Sato, N. Nakajima and S. Ojita, *Tetrahedron Lett.*, 2009, **50**, 4751-4753.
- R. R. Gowda and E. Y. X. Chen, *Encyclopedia of Polymer Science and Technology*, 2013, 1-37.
- C. Hutchinson and E. Leete, *J. Chem. Soc. D: Chem. Commun.*, 1970, **0**, 1189-1190.
- L. E. Manzer, *Appl. Catal., A*, 2004, **272**, 249-256.
- M. K. Akkapaddi, *Macromolecules*, 1979, **22**, 546-551.
- J. Suenaga, D. M. Sutherland and J. Stille, *Macromolecules*, 1984, **17**, 2913-2916.
- M. Ueda and M. Takahashi, *J. Polym. Sci.*, 1982, **20**, 2819-2828.
- R. A. Cockburn, T. F. McKenna and R. A. Hutchinson, *Macromolecules*, 2010, **211**, 501-509.
- B. Mullen, M. Rodwogin, F. Stollmaier, D. Yontz and D. Leibig, *Green Materials*, 2013, **1**, 186-190.

- 20 J. Kollár, M. Mrlík, D. Moravčíková, Z. Kroneková, T. Liptaj, I. Lacík and J. Mosnáček, *Macromolecules*, 2016, **49**, 4047-4056.
- 21 C. Preusser and R. A. Hutchinson, *Macromol. Symp.*, 2013, **333**, 122-137.
- 22 M. Buback, R. G. Gilbert, R. A. Hutchinson, B. Klumperman, F.-D. Kuchta, B. G. Manders, K. F. O'Driscoll, G. T. Russell and J. Schweer, *Macromol. Chem. Phys.*, 1995, **196**, 3267-3280.
- 23 I. Lacík, S. Beuermann and M. Buback, *Macromolecules*, 2003, **36**, 9355-9363.
- 24 I. Lacík, S. Beuermann and M. Buback, *Macromol. Chem. Phys.*, 2004, **205**, 1080-1087.
- 25 S. Beuermann, M. Buback, P. Hesse and I. Lacík, *Macromolecules*, 2006, **39**, 184-193.
- 26 I. Lacík, L. Ucnova, S. Kukuckova, M. Buback, P. Hesse and S. Beuermann, *Macromolecules*, 2009, **42**, 7753-7761.
- 27 I. Lacík, A. Chovancová, L. Uhelská, C. Preusser, R. A. Hutchinson and M. Buback, *Macromolecules*, 2016, **49**, 3244-3253.
- 28 F. D. Kuchta, A. M. van Herk and A. L. German, *Macromolecules*, 2000, **33**, 3641-3649.
- 29 D. L. Safranski and K. Gall, *Polymer*, 2008, **49**, 4446-4455.
- 30 J. Trompette, E. Fabregue and G. Cassanas, *J. Poly. Sci., Part B: Polym. Phys.*, 1997, **35**, 2535-2541.
- 31 W. F. Lee and P. L. Yeh, *J. Appl. Poly. Sci.*, 1997, **64**, 2371-2380.
- 32 Q. Tang, J. Wu, J. Lin, Q. Li and S. Fan, *J. Mater. Sci.*, 2008, **43**, 5884-5890.
- 33 C. E. Kadow, P. C. Georges, P. A. Jamney and K. A. Beningo, *Methods Cell Biol.*, 2007, **83**, 29-46.
- 34 S. He, F. Zhang and W. Wang, *Sustain. Chem. Eng.*, 2016, **4**, 3948-3959.
- 35 S. Beuermann, M. Buback, T. P. Davis, R. G. Gilbert, R. A. Hutchinson, O. F. Olaj, G. T. Russell, J. Schweer and A. M. van Herk, *Macromol. Chem. Phys.*, 1997, **198**, 1545-1560.
- 36 J. M. Asua, S. Beuermann, M. Buback, P. Castignolles, B. Charleux, R. G. Gilbert, R. A. Hutchinson, J. R. Leiza, A. N. Nikitin, J. P. Vairon and A. M. van Herk, *Macromol. Chem. Phys.*, 2004, **205**, 2151-2160.



80x26mm (150 x 150 DPI)